Gold supported on surface acidity modified Y-type and iron/Y-type zeolite for CO oxidation

Jiunn-Nan Lin, Jen-Ho Chen, Chih-Yang Hsiao, Yih-Ming Kang, Ben-Zu Wan*

Department of Chemical Engineering, National Taiwan University, Taipei 106, Taiwan, ROC

Abstract

A modified method for the preparation of gold in Y-type zeolite was developed in this research. Prior to the preparation of gold catalysts, the surface property of the zeolite (with or without iron) was adjusted in a 1 N sodium nitrate solution at pH 6. After drying, the zeolite was added into a chloroauric acid solution at pH 6 for gold loading. The resulted catalysts (i.e. Au/Y or Au/Fe/Y) possessed much better activity and stability for CO oxidation than those (i.e. Au/Y(NP) or Au/Fe/Y(NP)) without any surface pretreatment. Transmission electron microscopy (TEM) and X-ray photoelectron spectroscopy (XPS) studies indicate that the gold particles in Au/Y are smaller and more uniformly distributed than those in Au/Y(NP). XPS and temperature-programmed reduction (TPR) results suggest the strong interaction between gold and iron in Y-type zeolite. Furthermore, it was found from this research that Au/Fe/Y had full initial activity for CO oxidation at $0\,^\circ C$ and Au/Y required an induction period to reach a comparable activity to Au/Fe/Y. However, the stability of the activated Au/Y was much better than that of Au/Fe/Y. It can be concluded from XPS results that the formation of carbonate-like species, which covered the active sites for CO oxidation, was the main cause for the deactivation of Au/Fe/Y. On the other hand, TEM study suggests that the sintering of nano-gold particles was the main reason for the slight deactivation of Au/Y. © 2002 Elsevier Science B.V. All rights reserved.

Keywords: Gold; Y-type zeolite; Iron; Iron oxide; CO oxidation; Surface acidity

1. Introduction

Gold did not attract much attention in heterogeneous catalysis because of its chemical inertness and the difficulty for obtaining highly dispersed samples. However, several years ago Haruta et al. [1–3] found when co-precipitation of gold with various metal oxides, the gold catalysts possessed a dramatic activity for low-temperature CO oxidation. They discovered that gold nanoparticles supported on Co_3O_4, Fe_2O_3, and TiO_2 oxides have exceptionally high activity for many reactions. It is believed that these are correlated with the support property, the preparation method, and particularly the size of the Au clusters [4]. Since then many studies have been devoted to prepare ultrafine gold particles on the surface of metal oxides [5–7] and zeolites [8–15] for various reactions over the last few years.

It has been studied that small gold particles can be stabilized via inserting gold into the cages of zeolites [8–15]. Different kinds of Au/Zeolites have been prepared for NO reduction and CO oxidation [8–13]. Ichikawa and coworkers [8–10] used Au_2Cl_6 as a precursor to prepared Au(I)/NaY via a solid–vapor reaction. Fraissard and coworkers [14–15] used $[Au(en)_2]Cl_3$ to prepare Au/NaHY via a cation exchange method. Nevertheless, these gold catalysts

---

* Corresponding author. Fax: +886-2-23623040.
E-mail address: benzuwan@ccms.ntu.edu.tw (B.-Z. Wan).

were contaminated by chloride residuals. An additional high temperature pretreatment was required to activate the catalyst, which resulted in sintering of gold particles. Kang and Wan [11–13] in our previous research, developed a more convenient method to prepare Au/Y and Au/Fe/Y (Y is the Y-type zeolite) in the chloroauric acid solution (HAuCl$_4$·3H$_2$O). It was found that the as-prepared Au/Y showed high initial activity for low temperature CO oxidation but poor stability. However, the as-prepared Au/Fe/Y showed almost no activity and it can possess catalytic activity only after high temperature reduction. The low activity of as-prepared Au/Fe/Y was also caused by the residual Cl$^-$ species.

From the later study in our laboratory [16,17], it was concluded that gold loading and CO oxidation activity over Au/Y and Au/Fe/Y were affected by the pH of chloroauric acid solution. It is preferred to prepare gold in Y-type zeolite in the solution with pH between 6 and 7. However, it was noticed that there is surface acidity on zeolite Y, which may not fit for loading the gold species. Therefore, before loading gold, an attempt was made in our laboratory to modify the surface acidity of the Y-type zeolite in a sodium nitrate solution at pH 6. Surprisingly, it was found that gold species prepared on these surface modified zeolites showed much higher activities and maintained better stability during CO oxidation. Therefore, in this paper the detailed procedures for the preparation of Au/Y and Au/Fe/Y by the modified method are reported. The catalysts are compared with those without surface modification. The results of the characterization by X-ray diffraction (XRD), X-ray photoelectron spectroscopy (XPS), transmission electron microscopy (TEM) and temperature-programmed reduction (TPR) are presented. It is believed that the effects of surface modification on Y-type zeolite for loading gold species and for CO oxidation can be better understood from this research.

2. Experimental

2.1. Catalysts

Y-type zeolite with Si:Al = 2.3, sodium loading = 3.4 wt.% from Conteka was calcined at 550 °C in air for 4 h (designated Y(NP)) before it was used in this research. Two kinds of Fe/Y were prepared in this study. Fe-imp/Y(NP) was prepared by the incipient-wetness impregnation of aqueous solution of Fe(NO$_3$)$_3$·9H$_2$O (Riedel-deHaen) into Y(NP). The impregnated sample was dried at 60 °C for 4 h, then calcined at 550 °C for 4 h in air. Fe-ion/Y(NP) was prepared by ion exchanging of Fe(NO$_3$)$_3$·P9H$_2$O with Y(NP) in the aqueous solution at ambient temperature for 6 h. After filtration and washing by deionized water, the sample was dried at 60 °C and calcined at 550 °C for 4 h in air. For the gold loading process, Y(NP), Fe-imp/Y(NP) or Fe-ion/Y(NP) was directly charged into the chloroauric acid solution (Merck), which was pre-adjusted to pH 6 by a NaOH solution for 2 days. After filtration, washing and drying, the resulted samples were designated as Au/Y(NP), Au/Fe-imp/Y(NP) or Au/Fe-ion/Y(NP). However, for the new process developed in this research, prior to the gold loading process, the supports (i.e. Y(NP), Fe-imp/Y(NP), and Fe-ion/Y(NP)) were put into a 1 N NaNO$_3$ solution and the solution pH was adjusted to 6 by a 1 N sodium hydroxide solution. After the equilibrium was reached (generally, it takes 2 days), the samples was filtered and dried at 60 °C. These samples were designated as Y, Fe-imp/Y and Fe-ion/Y. Then the samples were for the following example process for loading gold: 4 g of Y, Fe-imp/Y or Fe-ion/Y was added into a 500 ml chloroauric acid solution (0.032 wt.% of Au, pH = 6). Under stirring, the solution was heated to 80 °C and maintained at this temperature for 16 h. After filtration, washing and drying, the as-prepared gold catalysts were designated as Au/Y, Au/Fe-imp/Y and Au/Fe-ion/Y. Because a question about why not adjusting the surface acidity of Y-type zeolite during the gold loading process was raised, the following procedures were used for preparing a reference sample: 4 g of Y(NP) was added into 500 ml of 0.032 wt.% of chloroauric acid solution (pH = 6). Under stirring, the pH of the solution was monitored and adjusted to pH 6.8 (which was the filtrate pH of Au/Y solution at the end of preparation) for the first half an hour at room temperature. Then the solution under the condition without adjusting pH was heated to 80 °C and maintained at this temperature for 16 h. After filtration, washing and drying, the as-prepared sample was designated as [Au/Y(NP)]$_{pH}$.

2.2. Characterization

The elemental content in each sample was determined by an AA unit (GBC 906) and by an ICP-AES unit (Kontro Plasmakon Model S-35). The zeta potential of the supports were measured by a Zetasizer 2000 (Malvern). The TEM pictures were taken using a Hitachi H7100 electron microscope operated at 75 kV. For the measurement of TPR, the experimental procedures and the apparatus were described in detail in [18]. The samples were purged in a carrier gas (mole ratio of $H_2:N_2 = 1:9$) of 30 ml/min flow rate at room temperature for 20 min before the measurement. For the measurement of binding energy, a PHI 1600 ESCA spectrometer, using Mg Kα monochromatic X-rays, was applied. All the measured binding energies (BE) were referred to the C 1s line at 284.6 eV. The XRD measurements were carried out by a MAC Science Diffractometer (Model MXP-3) with Cu Kα radiation at 40 kV and 30 mA.

2.3. Catalytic activity

Carbon monoxide oxidation was carried out in a quartz-tubular reactor (7 mm i.d.) under atmospheric pressure. The catalysts, which contained a fixed amount of gold, were used for the reaction. 32.7 ml/min of air and 0.33 ml/min of carbon monoxide (99.3%, CP grade, Linde Division, Union Carbide) were purified by 4 Å molecular sieves, then mixed and flowed into the reactor for the reaction. Shimadzu GC-8A gas chromatograph was used for the analysis of the composition in the reactor outstream. A Carboxy-2000 column was applied for the separation of carbon dioxide, carbon monoxide, nitrogen and oxygen.

3. Results and discussions

3.1. Metal loading and CO conversion over Au/Y(NP), Au/Y and [Au/Y(NP)]$_{pH}$

Table 1 lists the metal loading in Au/Y(NP), Au/Y, [Au/Y(NP)]$_{pH}$ and in each supports before loading gold. For Y-type zeolite, the amount of aluminum is decreased with an increase of sodium after the surface modification. It is because some of aluminum in

Table 1
Metal loadings in Y-type zeolites

Catalyst	Metal loading (wt.%)				pH of filtrate[a]
	Au	Fe	Al	Na	
Y(NP)	–	–	14.4	3.4	–
Y	–	–	12.6	5.1	–
Au/Y(NP)	1.59	–	12.8	2.4	6.7
Au/Y	1.70	–	12.4	3.0	6.8
[Au/Y(NP)]$_{pH}$	0.90	–	12.7	2.5	7.0
Fe-imp/Y	–	3.82	12.5	–	–
Fe-ion/Y	–	4.45	8.8	–	–
Au/Fe-imp/Y	3.56	3.61	12.2	–	6.7
Au/Fe-ion/Y	3.62	4.21	8.7	–	6.4

[a] pH of the filtrate after the process of loading gold in the chloroauric acid solution.

Y-type zeolite was leached out and some of the proton on the ion exchange sites in Y-type zeolite was exchanged by sodium ions in the 1 N NaNO$_3$ solution. The XRD results showed that all the structures of Y-type catalysts were maintained after surface modification. Thus, it is suggested that the modification of Y-type zeolite only caused a change of the surface properties and there was no significant collaps e of the zeolite structure. Interestingly, it can be found in Table 1 that the gold loading in Au/Y is higher than that in Au/Y(NP), and the pH values of the filtrates after the preparation of gold in Au/Y and Au/Y(NP) are in a close range. This indicates that the gold species in the solutions for the preparation of these two catalysts were similar. The different surface property of Y and Y(NP) caused different gold loadings in Au/Y and Au/Y(NP). Therefore, if there are any more different physical or catalytic properties of these two in the later studies, it should be from the effect of surface property during gold loading process.

Fig. 1 shows the experimental results of CO conversions over as-prepared Au/Y(NP), Au/Y and [Au/Y(NP)]$_{pH}$ catalysts (each contained 0.0006 g of Au) at 40 °C. It was found that Au/Y, shown in Fig. 1a, from surface modified Y maintained a CO conversion close to 99% for at least 48 h. Nevertheless, Au/Y(NP), shown in Fig. 1b, had an initial conversion of 66%. Its catalytic activity decayed rapidly at the first 5 h, then to a CO conversion of 38% after 48 h. [Au/Y(NP)]$_{pH}$ in Fig. 1c showed the lowest CO conversion among these three catalysts. It had very low initial activity and then reached a conversion of 15%
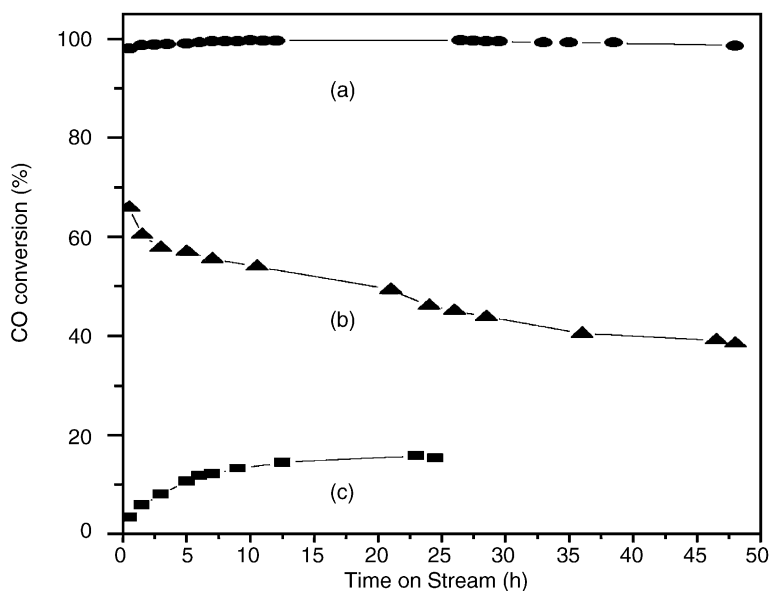
Fig. 1. CO conversion vs. time on stream at 40 °C over (a) Au/Y, (b) Au/Y(NP), and (c) [Au/Y(NP)]$_{pH}$, which contained 0.0006 g of gold.

after 24 h. From these results, it can be concluded that the surface modification process for Y-type zeolite used in this research is an effective way to enhance the catalytic property of Au/Y for CO oxidation. However, by adjusting the solution pH during gold loading process, i.e. for making [Au/Y(NP)]$_{pH}$, is not effective for improving the catalytic property; in fact, it is worse than without.

3.2. TEM and zeta potential of Au/Y(NP), Au/Y and [Au/Y(NP)]$_{pH}$

In order to understand why Au/Y(NP), Au/Y and [Au/Y(NP)]$_{pH}$ possess different catalytic properties, TEM experiments were carried out. Fig. 2 shows the results. It can be observed that there are two kinds of gold particles on or in both Au/Y(NP) and Au/Y. One is from large particles on the external surface of the supports, the other is from small nanoparticles within the cages. For Au/Y(NP), the large gold particles (in Fig. 2a) are between 10 and 15 nm, which are much larger than those (shown in Fig. 2b) around 5 nm on Au/Y. The smaller gold particles in both Au/Y(NP) and Au/Y are <2 nm. However, most gold particles on [Au/Y(NP)]$_{pH}$ are larger than 20 nm as shown

in Fig. 2c. The larger gold particles would provide less surface area for the reaction. Therefore, the gold particle sizes observed from TEM have given a good explanation why [Au/Y(NP)]$_{pH}$ had the lowest CO conversion, and why the CO conversion over Au/Y was higher and more stable than that over Au/Y(NP).

The zeta potential can represent the amount of surface charges on Y(NP) and Y. The zeta potential is −3 mV on Y(NP) and is −10 mV on Y at pH 6. These negative charges can prevent vigorous deposition of gold species with negative charges, such as Au(OH)$_{4-x}$Cl$_x^-$, on the surface of zeolites. Since there are more negative charges on Y than those on Y(NP), the deposition of negative gold species on Y should be less than those on Y(NP). This may be one of the reasons why the gold particle sizes on the external surface of Au/Y is smaller than those of Au/Y(NP). Nevertheless, if the deposition of negative gold species were the only path for loading gold species on Y-type zeolite, the gold loading in Au/Y(NP) should have been higher than that in Au/Y. In fact, it is just the opposite as shown in the data of Table 1. Therefore, there must be some other paths (e.g. cation deposition or cation exchange) for loading gold species in Y-type zeolite in the solution.
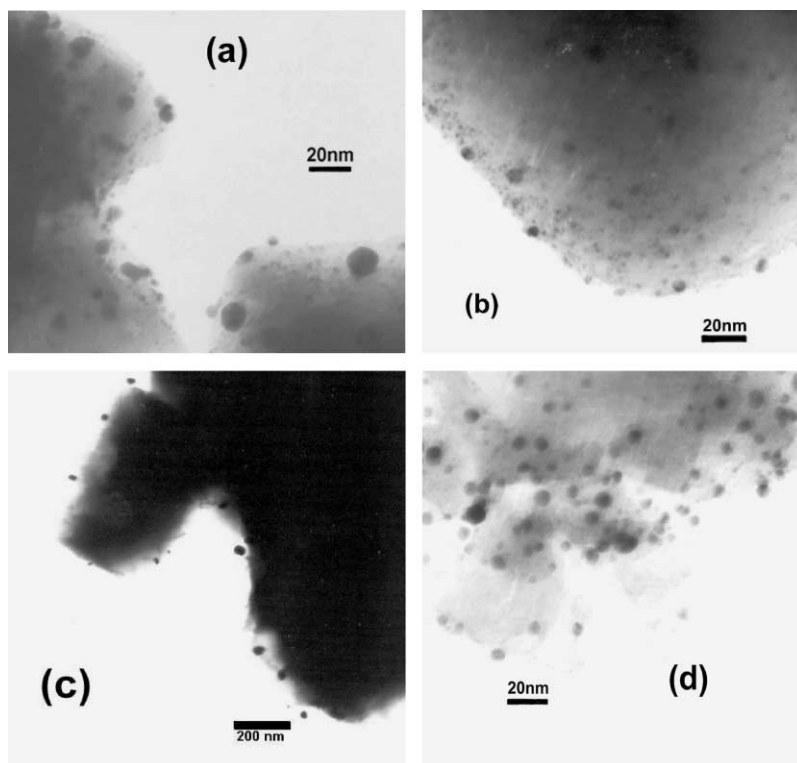
Fig. 2. TEM photographs of (a) Au/Y(NP) (b) Au/Y, (c) [Au/Y(NP)]$_{pH}$, and (d) Au/Y after CO reaction.

Although the solution pH of [Au/ Y(NP)]$_{pH}$ was adjusted to pH 6.8, which was the same pH value at the end of preparation process for Au/ Y, the gold particle sizes and the gold loading on [Au/Y(NP)]$_{pH}$ were not close to those on Au/ Y. [Au/ Y(NP)]$_{pH}$ possesses a much lower gold loading, 0.9 wt.%, and much larger gold particles than Au/ Y. This indicates that this solution adjustment only mainly changed the pH of the gold solution. The limited adjustment time was not sufficient to change the surface properties of Y(NP) to Y (note, it took 2 days to prepare Y from Y(NP) as illustrated in Section 2). However, the higher solution pH for [Au/ Y(NP)]$_{pH}$ produced more gold hydroxide, Au(OH)$_3$ and Au(OH)$_3$Cl$^-$. These gold species formed larger gold particles in the solution via a condensation process of the hydroxyl groups. Some of them would be too large to access into the cages of zeolite. Therefore, for [Au/ Y(NP)]$_{pH}$, the gold loading was less and the gold particles were larger than those on Au/ Y and Au/ Y(NP).

3.3. XPS spectra over Au/Y(NP), Au/Y and [Au/Y(NP)]$_{pH}$

The spectra corresponding to gold are shown in Fig. 3. It can be observed that there are several gold species on these catalysts. After deconvolution, the fitting results are listed in Table 2. The gold species can be classified into metallic gold (Au) and ionic gold (Au^{3+}). For Au^{3+} on Au/Y, shown in Fig. 3a, at least two different gold species can be observed. One is Au(OH)$_2$$^+$ and the other is Au$_2$O$_3$ gold dimers. However, for Au^{3+} on Au/Y(NP) and [Au/Y(NP)]$_{pH}$, shown in Fig. 3b and c, only Au$_2$O$_3$ is found. It is noticed that the BE of Au$_2$O$_3$ from this research is very close to that in Au/Fe$_2$O$_3$ and Au/Al$_2$O$_3$ [19]. Nevertheless, the BE of Au(OH)$_2$$^+$ is higher than that of Au(OH)$_3$ in Au/Al$_2$O$_3$ by about 0.5 eV [19]. This is reasonable because gold in cationic gold hydroxides certainly possess higher BE than that in the neutral gold hydroxide. On the other hand, for metallic Au,
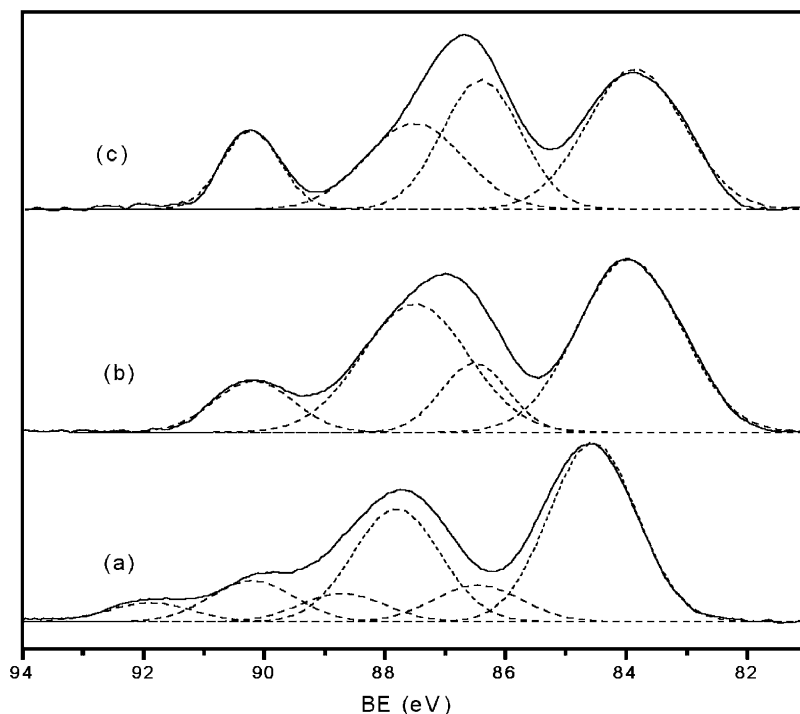
Fig. 3. XPS spectra of (a) Au/Y (b) Au/Y(NP), and (c) [Au/Y(NP)]$_{pH}$. All the catalysts were dried at room temperature.

it is noticed that BE of the three gold catalysts, listed in Table 2, are different. The BE of metallic gold on Au/Y catalysts is higher than those on Au/Y(NP) and [Au/Y(NP)]$_{pH}$, which show BE values similar to that of bulk gold (BE < 84 eV) [20]. This suggests the existence of small gold metal clusters in Au/Y, because Rao et al. [21] have observed similar BE shifts of the Au 4f lines of the small gold clusters. In general, small gold clusters with a mean diameter <2 nm show

significantly larger BE than the bulk gold metal. Therefore, the gold particles in Au/Y should be smaller than 2 nm from our XPS study. This result is consistent with that observed from the TEM photographs. Moreover, Table 2 lists the XPS peak widths (full-widths at half-maximum band intensity, FWHM) of metallic gold. It can be found that FWHM from Au/Y(NP), 1.7 eV, and that from [Au/Y(NP)]$_{pH}$, 1.6 eV, are larger than that from Au/Y, 1.4 eV. These results indicate

Table 2
Binding energies of Au $4f_{7/2}$ on Au/Y, Au/Y(NP) and [Au/Y(NP)]$_{pH}$

Catalysts[a]	Au $4f_{7/2}$ (eV)			Peak area ratio (Au:Au^{3+})	FWHM[b] of metallic gold
	Au	Au^{3+}			
		Au_2O_3	$Au(OH)_2{}^+$		
Au/Y	84.4	86.4	88.2	2.0	1.4
Au/Y(NP)	84.0	86.5		3.7	1.7
[Au/Y(NP)]$_{pH}$	83.9	86.4		1.5	1.6

[a] All the samples were dried at room temperature.

[b] Full-widths at half-maximum intensities.

that there are wider-spreading small and large metallic gold particles on Au/Y(NP) and [Au/Y(NP)]$_{pH}$. The metallic gold particles in Au/Y are more uniformly distributed. This is also consistent with the TEM results.

During the process for loading gold on Y(NP) and Y in a dilute chloroauric acid solution in this research, since similar solution pHs were monitored, therefore, it is thought that Au(OH)$_2{}^+$, Au$_2$O$_3$ (gold dimers) and gold metals should have been prepared on Au/Y(NP) and Au/Y. In fact, only XPS results from Au/Y showed Au^{3+} bands corresponding to Au(OH)$_2{}^+$ and Au$_2$O$_3$; those from Au/Y(NP) showed the only Au^{3+} band corresponding to Au$_2$O$_3$. The disappearance of Au(OH)$_2{}^+$ on Au/Y(NP) suggests that the transformation of Au(OH)$_2{}^+$ to Au$_2$O$_3$ was faster on Au/Y(NP) than on Au/Y. This is attributed to the different surface properties of Au/Y(NP) and Au/Y. Since the surface of Y(NP) is not modified before gold loading, there are more H$^+$ on Au/Y(NP) than that on Au/Y. Apparently, H$^+$ on the surface is the catalyst for the dehydration (or condensation) surface reaction of Au(OH)$_2{}^+$ to Au$_2$O$_3$ of gold dimers. Furthermore, it is believed that H$^+$ is also responsible for catalyzing the deep condensation reactions of gold ion species on the surface. There may be several Au(OH)$_2{}^+$ to react sequentially to form large gold oxide particles. Therefore, although the total gold loading on Au/Y(NP) was less than that on Au/Y, the sequential condensation reactions can cause the gold particle sizes on Au/Y(NP) being larger than those on Au/Y.

Table 2 also lists the peak area ratio of Au:Au^{3+} of each catalyst. The data indicate that the ratio of Au:Au^{3+} from Au/Y is less than that from Au/Y(NP). It suggests that the formation rate of metallic gold on the surface of Au/Y is slower than that on Au/Y(NP). Nevertheless, as shown in Table 2, the ratio of Au:Au^{3+} on [Au/Y(NP)]$_{pH}$ is the least among these three gold catalysts. It has been discussed in the previous sections that [Au/Y(NP)]$_{pH}$ was prepared in the solution with higher pH than Au/Y and Au/Y(NP). More large gold species were formed and deposited on [Au/Y(NP)]$_{pH}$. Apparently, these large gold species are not in metallic form and it takes time to transform them to gold metal at room temperature. Therefore, [Au/Y(NP)]$_{pH}$ possesses the least ratio of Au:Au^{3+}.

3.4. Metal loading and CO oxidation over Au/Fe-imp/Y and Au/Fe-ion/Y

The effects of surface modification on iron Y-type zeolite for loading gold and for catalytic CO oxidation were also investigated in this research. Table 1 lists the metal loadings in Fe-imp/Y, Fe-ion/Y, Au/Fe-imp/Y and Au/Fe-ion/Y. It can be found that a significant amount of aluminum was leached out from Y-type zeolite during iron ion exchange process, due to the low pH of the solution. After preparing gold into Y, Fe-imp/Y and Fe-ion/Y, the gold loadings in Au/Fe-imp/Y and Au/Fe-ion/Y were two times more than that in Au/Y. Solution chemistry has shown that colloidal gold and complexed gold (AuCl$_{4-x}$(OH)$_x{}^-$) can react with the forming iron oxide surfaces [22]. The iron sites (in the form of iron cation and iron oxides) on Fe/Y were also the sites for Au deposition, since the surface of iron oxide (with an isoelectric point around pH 7.0) was positively charged during the gold loading process. Therefore, the presence of iron in Y-type zeolite enhanced the gold loading. XRD patterns showed that all the structures of Y-type zeolite were maintained after the preparation of Au/Fe/Y.

Fig. 4 shows the carbon monoxide conversions over Au/Y, Au/Fe-imp/Y and Au/Fe-ion/Y at 0 °C. All the catalysts were dried at 60 °C under air before the reactions. It can be observed that both Au/Fe-imp/Y and Au/Fe-ion/Y showed high initial activities. The results were different from those over Au/Fe-imp/Y(NP) and Au/Fe-ion/Y(NP) reported in our previous research [13], in which Au/Fe/Y(NP) samples possessed almost no catalytic activity for CO oxidation at reaction temperature as high as 40 °C. Apparently, the surface modification process for Fe-imp/Y and Fe-ion/Y developed in this research is effective for preparing highly active gold and iron supported on Y-type zeolite.

3.5. Characterization of Au/Y and Au/Fe/Y by TPR and XPS

Fig. 5 shows the TPR profiles of Fe/Y, Au/Y and Au/Fe/Y. It can be observed that the reduction temperature from Fe-imp/Y is around 450 °C. It is higher than that from Fe-ion/Y by 62 °C. This indicates that it is easier to reduce iron ions in Fe-ion/Y than iron oxides in Fe-imp/Y. After the preparation of Au in surface modified Fe/Y to form Au/Fe-imp/Y
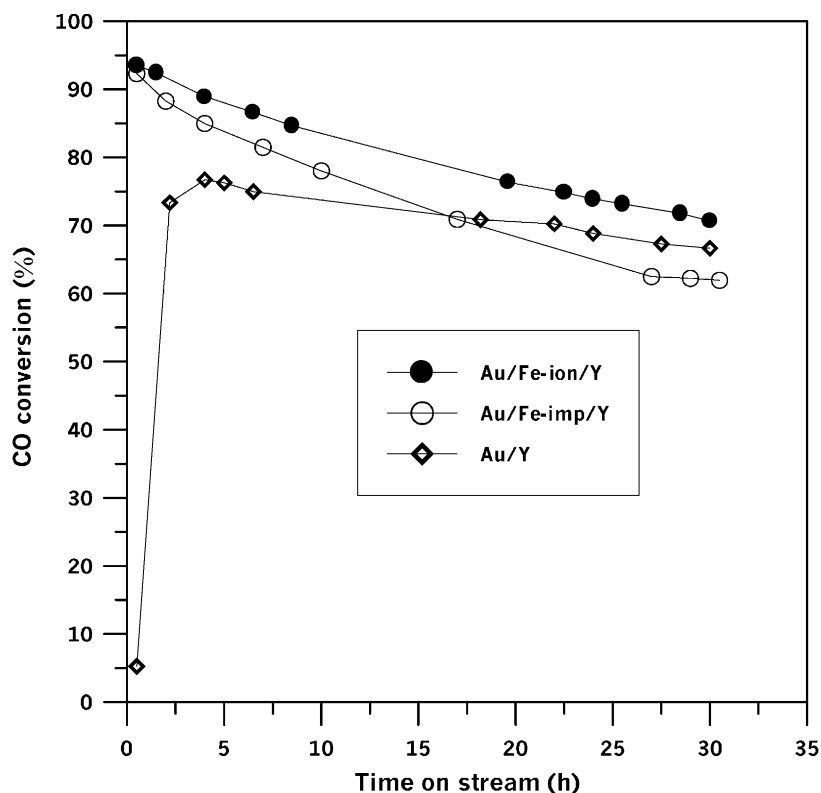
Fig. 4. CO conversion vs. time on stream at $0\,°C$ over Au/Y and Au/Fe/Y. Each catalyst contained $0.0006\,g$ of gold and was dried at $60\,°C$ under air before the reaction.

and Au/Fe-ion/Y, most of the reduction temperatures were dropped to around $100\,°C$, which were about $50\,°C$ lower than those from Au/Fe-imp/Y(NP) and Au/Fe-ion/Y(NP) prepared in the previous research [13]. This suggests that Au/Fe-imp/Y and Au/Fe-ion/Y prepared from this research are easier applied for the oxidation–reduction catalytic reactions than Au/Fe-imp/Y(NP) and Au/Fe-ion/Y(NP). Moreover, it is noticed in Fig. 5 that there are single reduction bands for Au/Y and Au/Fe-ion/Y around $100\,°C$. Nevertheless, there are two separable reduction bands at 101 and $125\,°C$ for Au/Fe-imp/Y, the former is from the reduction of gold ions and the latter is from the reduction of gold–iron mixed oxides. This indicates that gold and iron oxides in Au/Fe-imp/Y are not uniformly interacted in Y-type zeolite. However, for Au/Fe-ion/Y, the single reduction band around $100\,°C$ indicates the uniform interaction between gold and iron ions.

Table 3 summarizes the BE of Au $4f_{7/2}$ and Fe $2p_{3/2}$ in Au/Y, Au/Fe-imp/Y and Au/Fe-ion/Y. Different from the samples dried at room temperature listed in Table 2, the samples in Table 3 were dried at $60\,°C$, prior to evacuation for XPS measurement. It was found from XPS that there was no BE corresponding to $Au(OH)_2{}^+$. There were only two Au $4f_{7/2}$ BE, around 84.4 and $86.5\,eV$, the former represents the BE of metallic gold and the latter represents the BE of ionic gold (Au_2O_3). Similar to the results of Au/Y in Table 2, higher BE of metallic gold than that (about $84\,eV$) of bulk gold can be observed in Table 3. It indicates the existence of small metallic gold in Au/Y, Au/Fe-imp/Y and Au/Fe-ion/Y. Therefore, similar to the nanoparticles sizes of gold samples in Table 2, the gold particle sizes in Au/Y, Au/Fe-imp/Y and Au/Fe-ion/Y after dried at $60\,°C$ are about $2\,nm$.

The BE of Au_2O_3 from Au/Fe-imp/Y and Au/Fe-ion/Y are higher than that from Au/Y, which
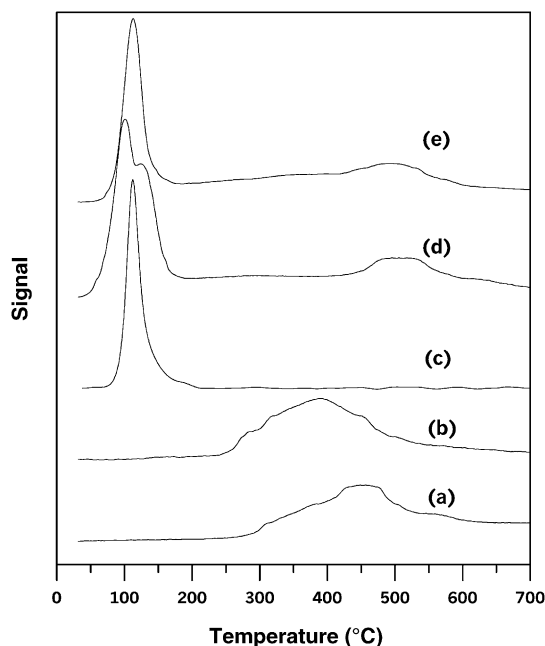
Fig. 5. TPR spectra of (a) Fe-imp/Y, (b) Fe-ion/Y, (c) Au/Y, (d) Au/Fe-imp/Y, and (e) Au/Fe-ion/Y.

indicates an interaction between gold and iron in Y-type zeolite. Because the interaction between gold and iron in Au/Fe-ion/Y is stronger than that in Au/Fe-imp/Y, iron ions in Au/Fe-ion/Y withdraw more electrons from gold species than iron oxides in Au/Fe-imp/Y. Therefore, it can be observed from Table 3 that the BE of Au 4f lines from Au/Fe-ion/Y

is higher than that from Au/Fe-imp/Y. Furthermore, the stronger interaction between gold and iron causes the less formation of metallic gold from ionic gold in Y-type zeolite. Therefore, it can be found in Table 3 that the peak area ratios of metallic gold to ionic gold of Au/Y, Au/Fe-imp/Y, and Au/Fe-ion/Y are 1.5, 1, and 0.25, respectively. Au/Y possessed the most metallic gold, and Au/Fe-ion/Y possessed the least.

Table 3 also lists the BE of Fe $2p_{3/2}$ in Au/Fe-imp/Y and Au/Fe-ion/Y. The BE of Fe $2p_{3/2}$ in Au/Fe-imp/Y and Au/Fe-ion/Y are 711.6 and 710.7 eV. It indicates that iron in Au/Fe-ion/Y is at a lower oxidation state than that in Au/Fe-imp/Y. These results are consistent with the previous discussion, while iron in Au/Fe/Y pull more electrons from gold than that in Au/Fe-imp/Y, due to stronger interaction between gold and iron in Au/Fe-ion/Y. Furthermore, it was reported that α-Fe$_2$O$_3$, FeO, Fe$_3$O$_4$, and FeOOH have Fe $2p_{3/2}$ BE values at 711.6, 709.6, 710.8 and 711.2 eV, respectively [23]. Therefore, it was Fe$_2$O$_3$ in Au/Fe-imp/Y; and it was iron ions (with an oxidation state similar to that of Fe in Fe$_3$O$_4$) in Au/Fe-ion/Y.

3.6. Comparison of CO oxidation activity over Au/Y and Au/Fe/Y

All the catalysts were dried under air at 60 °C prior to the reaction tests. The reaction results of CO oxidation at 0 °C, as shown in Fig. 4, present that the initial catalytic activity of Au/Y and Au/Fe/Y are different. For both Au/Fe-ion/Y and Au/Fe-imp/Y, the initial high CO conversions (more than 90%) were

Table 3
Binding energies of Au 4f$_{7/2}$ and Fe 2p$_{3/2}$ on Au/Y and Au/Fe/Y after dried in air at 60 °C

Catalyst[a]	Au 4f$_{7/2}$ (eV)		Fe 2p$_{3/2}$ (eV)	Peak area ratio			
	Au	Au$_2$O$_3$		Au:Au^{3+}	Cl:Au$_t$[d]	Au$_t$:Fe	C:Au$_t$
Au/Y	84.4	86.5	–	1.5	1.5	–	14
	83.8[b]	–	–	0.0	–	–	
	84.0[c]	–	–	0.0	–	15	
Au/Fe-imp/Y	84.4	86.6	711.6	1.0	1.5	1.6	15
	84.1[c]	711.2	–	0.0	0.7	240	
Au/Fe-ion/Y	84.7	86.8	710.7	0.25	1.2	0.7	–

[a] All the samples were dried in air at 60 °C prior to evacuation for XPS measurement.
[b] After TPR in H$_2$:N$_2$ = 1:9 until 800 °C.
[c] After CO oxidation at 0 °C for 30 h.
[d] Au$_t$: the sum of XPS area of total gold (Au and Au^{3+}).

obtained. Nevertheless, there was almost no initial activity for Au/Y. It can be activated and reached a 75% CO conversion after an induction period of about 4 h at 0 °C. However, the stability of Au/Y after activation was better than that of Au/Fe/Y catalysts. It can be observed from Fig. 4 that the activity decaying rates of Au/Fe/Y are higher than that of Au/Y. After reaction time on stream for 30 h, it was observed that the activity of Au/Y had been higher than that of Au/Fe-imp/Y and slightly less than that of Au/Fe-ion/Y.

From the gold solution chemistry [24], it was found that $AuCl_2(OH)_2^-$ and $AuCl(OH)_3^-$ were the predominant gold complexes in the pH range of 6–7 at a transient state. Therefore, it was inevitable to possess some chloride ions over these gold catalysts. As shown XPS results in Table 3, all the gold catalysts contained a Cl:Au ratio around 1.5 and these residual surface chloride ions were not detected on the catalysts after CO reaction. The nearly no initial activity of Au/Y at 0 °C may be from that its surface was covered with some chloride ions. For Au/Y, therefore, it took a period of initiation time to remove these surface chlorides. However, Au/Fe/Y did not need any initiation time for CO oxidation at 0 °C. The co-existence of iron in Au/Fe/Y might help to remove the chloride ions from gold species more easily.

The reaction mechanisms for CO oxidation over gold catalyst are still under discussion. It was concluded that the catalytic CO oxidation mechanism over Au/Fe_2O_3 [25–26] was different from that over Au/TiO_2 [27] and polycrystalline gold [28]. For Au/Fe_2O_3, it was shown that iron oxide was the oxygen provider for the reaction. And the reaction mechanism involves the removal and replenishment of lattice oxygen, where the presence of gold promotes these processes. For Au/TiO_2 and polycrystalline gold, the CO oxidation occurred via a Langmuir–Hinshelwood (L–H)-type mechanism, i.e. simultaneous adsorption and reaction of CO and O at gold sites. However, Boccuzzi et al. [29] suggested that two independent pathways might exist for the reaction. One occurred rapidly and directly at the surface of the metallic gold particles and the other was slower and induced by the oxygen in the gas phase, involving the surface lattice oxygen of the supports and of the borderline with the gold particles. Therefore,

the CO reaction over Au/Y could be via an L–H-type mechanism since gold particles were the only possible active sites for CO oxidation and the dissociative adsorption of oxygen was the rate-determining-step (RDS) for CO oxidation, which was easily inhibited by chloride ions. The CO oxidation over Au/Fe/Y could be via the two independent reaction pathways [29]. This may be one of the reasons that the initial CO conversions over Au/Fe/Y were higher than that over Au/Y.

Furthermore, for Au/Fe/Y catalysts, the more the interaction between gold and iron over Au/Fe/Y, the more peripheries can be provided for CO oxidation. XPS results in Table 3 showed that the Au:Fe ratio of Au/Fe-imp/Y (1.6) was two times larger than that of Au/Fe-ion/Y (0.7). This suggests that there were more peripheries existed per unit mass gold particles over Au/Fe-ion/Y. This is consistent with the TPR results. Therefore, the difference between Au/Fe-imp/Y and Au/Fe-ion/Y for CO oxidation was due to the different dispersions of gold species over Au/Fe/Y catalysts.

However, the catalytic activity of Au/Fe/Y decayed more rapidly than Au/Y. It was observed from XPS that the C:Au ratio increased enormously in Au/Fe-imp/Y catalyst after CO oxidation and the Au:Fe ratio of Au/Fe-imp/Y was also decreased after reaction, as shown in Table 3. Many groups have found that the presence of carbonate-like species occurred during CO oxidation [25–28]. These species were stable below 100 °C [25], which were regarded as by-products that were not important for CO_2 formation and probably inhibit the reaction of CO oxidation. It was also observed by Kang and Wan [12] that the deactivation over Au/Fe/Y could be recovered by a thermal treatment under inert gas. Thus, the accumulation of these carbonate-like species over gold–iron peripheries could contribute for the deactivation of Au/Fe/Y catalysts. As the reaction goes further, the carbonate-like species can accumulate more to cover the gold surface, which results in the further deactivation of Au/Fe/Y. Finally, gold particles were the only active sites remained for CO oxidation over Au/Fe/Y. Therefore, the activity of Au/Y had been higher than that of Au/Fe-imp/Y, and slightly less than that of Au/Fe-ion/Y after CO reaction for 30 h.

The deactivation of Au/Y for CO reaction was different from Au/Fe/Y. The C:Au ratios over Au/Y, listed

in Table 3, only increased a little after the reaction. Thus, the decrease of CO activity over Au/Y was not likely from the accumulation of carbon coke. It was also indicated in Table 3 that there was only one binding energy of Au $4f_{7/2}$, designated as metallic gold over Au/Y catalyst after CO oxidation and it was close to the BE of Au $4f_{7/2}$ of bulk gold metals. The TEM results in Fig. 2d showed gold particles in Au/Y sintered after CO oxidation. Therefore, the slight decrease of CO conversion over Au/Y was predominantly from the sintering of nano-gold particles in Y-type zeolite.

4. Conclusions

1. Both Au/Y and Au/Fe/Y prepared in this research had much higher catalytic activity for CO oxidation than those (Au/Y(NP) and Au/Fe/Y(NP)) prepared from our previous research [11–13].
2. Au/Fe/Y had very high initial activity for CO oxidation, however, Au/Y needed an induction period to be fully activated for CO oxidation at $0\,°C$. After fully activated, Au/Y possessed similar activity but much better stability than Au/Fe/Y.
3. TEM showed that the gold particles size on Au/Y was smaller and more uniform distributed than Au/Y(NP).
4. From XPS study, $Au(OH)_2{}^+$ which has binding energy higher than $Au(OH)_3$ by about $0.5\,eV$ was observed on Au/Y; however, it was not observed on Au/Y(NP).
5. The formation of carbonate-like species, which blocked the active sites for CO oxidation, was the main reason for the deactivation of Au/Fe/Y. On the other hand, the sintering of gold nanoparticles on Au/Y was the main reason for the slight deactivation of Au/Y after initiation.
6. There was a strong interaction between gold and iron in Au/Fe/Y, which was evidenced by XPS and TPR experiments.

Acknowledgements

References

[1] M. Haruta, T. Kobayashi, H. Sano, N. Yamada, Chem. Lett. (1987) 405.
[2] M. Haruta, N. Yamada, T. Kobayashi, S. Iijima, J. Catal. 115 (1989) 301.
[3] M. Haruta, S. Tsubota, T. Kobayashi, H. Kageyama, M.J. Genet, B. Delmon, J. Catal. 144 (1993) 175.
[4] G.C. Bond, D.T. Thompson, Catal. Rev. Sci. Eng. 41 (1999) 319.
[5] A. Knell, P. Barnickel, A. Baiker, A. Wokaun, J. Catal. 137 (1992) 306.
[6] S.D. Lin, M. Bollinger, M.A. Vannice, Catal. Lett. 17 (1993) 245.
[7] M.C. Kung, J.-H. Lee, A. Chu-Kung, H.H. Kung, Stud. Surf. Sci. Catal. 101 (1996) 701.
[8] S. Qiu, R. Ohnishi, M. Ichikawa, J. Phys. Chem. 101 (1994) 2719.
[9] T.M. Salama, T. Shido, H. Minagawa, M. Ichikawa, J. Catal. 152 (1995) 322.
[10] T.M. Salama, R. Ohnishi, M. Ichikawa, J. Chem. Soc., Faraday Trans. 92 (1996) 301.
[11] Y.M. Kang, B.Z. Wan, Appl. Catal. A: Gen. 128 (1995) 53.
[12] Y.-M. Kang, B.-Z. Wan, Catal. Today 26 (1995) 59.
[13] Y.-M. Kang, B.-Z. Wan, Catal. Today 35 (1997) 379.
[14] D. Guillemot, M. Polisset-Thfoin, J. Fraissard, Catal. Lett. 41 (1996) 143.
[15] V.Y. Borovkov, V.B. Kazansky, M. Polisset-Thfoin, J. Fraissard, J. Chem. Soc., Faraday Trans. 93 (1997) 3587.
[16] C.-Y. Hsiao, Improvement and study of gold iron oxide catalysts for carbon monoxide oxidation, M.S. thesis, National Taiwan University, Taiwan, 1994.
[17] J.-H Chen, Redox behavior and catalytic carbon monoxide oxidation of gold/transition metal (3D) zeolite catalysts, M.S. thesis, National Taiwan University, Taiwan, 1996.
[18] Y.-M. Kang, B.-Z. Wan, Appl. Catal. A 114 (1994) 35.
[19] E.D. Park, J.S. Lee, J. Catal. 186 (1999) 1.
[20] C.D. Wagner, W.M. Riggs, L.E. Davis, J.M. Moulder, G.E. Muilenberg, Handbook of X-ray Photoelectron Spectroscopy, Perkin-Elmer, Eden Prairie, 1979.
[21] C.N.R. Rao, V. Vijayakrishnan, H.N. Aiyer, G.U. Kulkarni, G.N. Subbanna, J. Phys. Chem. 97 (1993) 11157.
[22] D.W. Thompson, I.R. Collins, J. Colloid Interface Sci. 152 (1991) 197.
[23] W.S. Epling, G.B. Hoflund, J.F. Weaver, S. Tsubata, M. Haruta, J. Phys. Chem. B 100 (1996) 9929.
[24] P.J. Murphy, M.S. LaGrange, Geochim. Cosmochim. Acta 62 (1998) 3515.
[25] A.K. Tripathi, V.S. Kamble, N.M. Gupta, J. Catal. 187 (1999) 332.
[26] M.M. Schubert, S. Hackenberg, C. van Veen, M. Muhler, V. Plzak, R.J. Behm, J. Catal. 197 (2001) 113.
[27] M.A. Bollinger, M.A. Vannice, Appl. Catal. B: Environ. 8 (1996) 417.
[28] N.M. Gupta, A.K. Tripathi, J. Catal. 187 (1999) 343.
[29] F. Boccuzzi, A. Chiorino, S. Tsubota, M. Haruta, J. Phys. Chem. 100 (1996) 3625.